Electronic Supplementary Material (ESI) for Chemical Science.

Supporting information

Chemoenzymatic Elaboration of the Raper-Mason Pathway Unravels the Structural Diversity within Eumelanin Pigments

Qing Zhe Ni, Brianna N. Sierra, James J. La Clair, Michael D. Burkart*

Department of Chemistry and Biochemistry, University of California, San Diego,
9500 Gilman Drive, La Jolla, California, 92093-0358, United States

*Correspondence and request for materials should be directed via email to
Michael D. Burkart (mburkart@ucsd.edu)

Contents: **Page**

A. General methods. Chemical reagents and enzymes were purchased from Worthington, Acros, Fluka, Sigma-Aldrich, or TCI. Deuterated NMR solvents were purchased from Cambridge Isotope Laboratories. All reactions were performed with stirring from Teflon coated stir bars using an IKAMAG RCT-basic mechanical stirrer (IKA GmbH). ^{1}H NMR spectra were recorded on 750 MHz Magnex Scientific magnet and Bruker spectrometer. Chemical shifts for ^{13}C NMR were referenced to the reported values of adamantine at 38.5 and 29.5 ppm. Chemical shift δ values for ^{1}H and ^{13}C spectra are reported in parts per million (ppm) relative to these referenced values. ChemDraw version 18 was utilized for all chemical shift predictions. All ^{13}C NMR spectra were recorded with complete proton decoupling. FID files were processed using TopSpin 3.2 (Bruker) and MestreNova 6.0.2 (Mestrelab Research). Scanning Electron Microscopy (SEM) analyses were performed using a FEI Quanta FEG 250 microscope (ThermoFisher Scientific) using a 3-5 kV energy source and a spot size of 3 under high vacuum at a working distance of 9 mm. Spectral data and procedures are provided for all new compounds and copies of select spectra have been provided.

B. General procedure for melanin polymerization. All precursor monomers were dissolved in 5 mM phosphate-buffered saline pH 7.5. Powdered mushroom tyrosinase I.U.B.1.14.18.1 (Worthington Biochemical) formula weight 128 kDa was added to the solution and stirred at 500-600 rpm for 24 h to 48 h at 23 °C. Solution color progressed from clear to pale yellow, followed by orange/brown and led to the final black solution.

C. General procedure for melanin isolation. The black solution was centrifuged at 4,500 rpm in MultifugeX3R (ThermoFisher Scientific), the supernatant was discarded, and the pellet was resuspended in H_2O (50 mL). The process was repeated 3-4 times until the supernatant became clear. The final pellet was then placed in a 1.9 mL tube (Eppendorf) to centrifuge at 13,000 rpm PrismR (Carolina Biological Supply Company). The supernatant was discarded and sample was dried by evaporation or via speed vacuum to remove residual water. Polymerization reactions were repeated to ensure reproducibility of the yields and improve the rigor of the protocols.

D. Polymerization reactions from single monomers. The following sections provide the methods for the preparation of each of the melanin samples in Figures 2-3.

L-Tyr-melanin. The reaction was conducted using the general procedure for melanin polymerization (section B) using L-tyrosine (L-Tyr, 1.0 g, 5.5 mmol) and mushroom tyrosinase (5.0 mg, 39.0 nmol) in 1.1 L of 5 mM phosphate-buffered saline pH 7.5. The solution was isolated using the general procedure (section C) to yield 109 mg (11%) of L-Tyr-melanin.

TA-melanin. The reaction was conducted using the general procedure for melanin polymerization (section B) using tyramine (TA, 754.5 mg, 5.5 mmol) and mushroom tyrosinase (5.0 mg, 39.0 nmol) in 1.1 L of 5 mM phosphate-buffered saline pH 7.5. The solution was isolated using the general procedure (section C) to yield 73 mg (10%) of TA-melanin.

L-DOPA-melanin. The reaction was conducted using the general procedure for melanin polymerization (section B) using L-DOPA (L-DOPA, 1.0 g, 5.1 mmol) and mushroom tyrosinase (5.0 mg, 39.0 nmol) in 1.1 L of 5 mM phosphate-buffered saline pH 7.5. The solution was isolated using the general procedure (section C) to yield 612 mg (61%) of L-DOPA-melanin.

DA-melanin. The reaction was conducted using the general procedure for melanin (section B) using dopamine • HCl (DA, 1.0 g, 5.1 mmol) and mushroom tyrosinase (5.0 mg, 39.0 nmol) in 1.1 L of 5 mM phosphate-buffered saline pH 7.5. The solution was isolated using the general procedure (section C) to yield 465 mg (46%) of DA-melanin.

4-HI-melanin. The reaction was conducted using the general procedure for melanin polymerization (section B) using 4-hydroxyindole (4-HI, 45.0 mg, 0.34 mmol) and mushroom

tyrosinase (2.0 mg, 15.6 nmol) in 100 mL of 5 mM phosphate-buffered saline pH 7.5. The solution was isolated using the general procedure (section C) to yield 16 mg (36%) of 4-HI-melanin.

5-HI-melanin. The reaction was conducted using the general procedure for melanin polymerization (section B) using 5-hydroxyindole (5-HI, 53.0 mg, 0.40 mmol) and mushroom tyrosinase (2.0 mg, 15.6 nmol) in 100 mL of 5 mM phosphate-buffered saline pH 7.5. The solution was isolated using the general procedure (section C) to yield 8.4 mg (16%) of 5-HI-melanin.

6-HI-melanin. The reaction was conducted using the general procedure for melanin polymerization (section B) using 6-hydroxyindole (6-HI, 45.0 mg, 0.34 mmol) and mushroom tyrosinase (2.0 mg, 15.6 nmol) in 100 mL of 5 mM phosphate-buffered saline pH 7.5. The solution was isolated using the general procedure (section C) to yield 21 mg (47%) of 6-HI-melanin.

7-HI-melanin. The reaction was conducted using the general procedure for melanin polymerization (section B) using 7-hydroxyindole (7-HI, 45.0 mg, 0.34 mmol) and mushroom tyrosinase (2.0 mg, 15.6 nmol) in 100 mL of 5 mM phosphate-buffered saline pH 7.5. The solution was isolated using the general procedure (section C) to yield 17 mg (38%) of 7-HI-melanin.

E. Polymerization reactions from monomer mixtures. The following sections provide the methods for the preparation of each of the melanin samples in Figure 4.

Melanised L-Tyr:TA. The reaction was conducted using the general procedure for melanin polymerization (section B) with L-Tyr (100.0 mg, 0.55 mmol), TA (100.0 mg, 0.73 mmol), and mushroom tyrosinase (2.0 mg, 15.6 nmol) in 200 mL of 5 mM phosphate-buffered saline pH 7.5. The solution was isolated using the general procedure (section C) to yield 11 mg (11%) of a L-Tyr/TA- mixed melanin polymer.

Melanised L-Tyr:L-DOPA. The reaction was conducted using the general procedure for melanin polymerization (section B) with L-Tyr (100.0 mg, 0.55 mmol), L-DOPA (100 mg, 0.51 mmol), and mushroom tyrosinase (2.0 mg, 15.6 nmol) in 200 mL of 5 mM phosphate-buffered saline pH 7.5. The solution was isolated using the general procedure (section C) to yield 53 mg (27%) of a L-Tyr/L-DOPA-mixed melanin polymer.

Melanised L-Tyr:DA. The reaction was conducted using the general procedure for melanin polymerization (section B) with L-Tyr (100.0 mg, 0.55 mmol), dopamine • HCl (100.0 mg, 0.53 mmol), and mushroom tyrosinase (2.0 mg, 15.6 nmol) in 200 mL of 5 mM phosphate-buffered saline pH 7.5. The solution was isolated using the general procedure (section C) to yield 38 mg (19%) of a L-Tyr/DA-mixed melanin polymer.

Melanised TA:L-DOPA. The reaction was conducted using the general procedure for melanin polymerization (section B) with TA (100.0 mg, 0.73 mmol), L-DOPA (100.0 mg, 0.51 mmol), and mushroom tyrosinase (2.0 mg, 15.6 nmol) in 200 mL of 5 mM phosphate-buffered saline pH 7.5. The solution was isolated using the general procedure (section C) to yield 118 mg (59%) of a TA/L-DOPA-mixed melanin polymer.

Melanised TA:DA. The reaction was conducted using the general procedure for melanin polymerization (section B) with TA (100.0 mg, 0.55 mmol), dopamine • HCl (100.0 mg, 0.53 mmol), and mushroom tyrosinase (2.0 mg, 15.6 nmol) in 200 mL of 5 mM phosphate-buffered saline pH 7.5. The solution was isolated using the general procedure (section C) to yield 71 mg (36%) of a TA/DA-mixed melanin polymer.

Melanised L-DOPA:DA. The reaction was conducted using the general procedure for melanin polymerization (section B) with L-DOPA (100.0 mg, 0.51 mmol), dopamine • HCl (100.0 mg, 0.53 mmol), and mushroom tyrosinase (2.0 mg, 15.6 nmol) in 200 mL of 5 mM phosphate-buffered saline pH 7.5. The solution was isolated using the general procedure (section C) to yield 156 mg (78%) of a L-DOPA/DA-mixed melanin polymer.

F. Polymerization reactions from isotopically-labeled monomers. The following sections provide the methods for the preparation of each of the melanin samples in Figure 5.

U-^{13}C,^{15}N L-Tyr-melanin. The reaction was conducted using the general procedure for melanin polymerization (section B) with U-^{13}C,^{15}N -L-tyrosine (100.0 mg, 0.52 mmol) and mushroom tyrosinase (2.0 mg, 15.6 nmol) in 110 mL of 5 mM phosphate-buffered saline pH 7.5. The solution was isolated using the general procedure (section C) to yield 35 mg (35%) of U-^{13}C,^{15}N-Tyr-melanin.

G. Solid state NMR (ss-NMR) spectroscopy. Dried natural abundance melanin sample (30 mg) was packed in 3.2 mm Bruker rotor. 1D ^{13}C CP spectra of the precursor monomers were acquired with 32 to 512 scans and a recycle delay of 3 s. Samples required 9k to 64k scans and were acquired with a recycle delay of 3 s. The CP contain times were optimized to 2 ms, with a ^{1}H decoupling of 83 kHz and a spinning frequency of 13.5 kHz. Data was acquired on a 750 ^{1}H MHz spectrometer (Bruker). Spinning sidebands from the NMR are labeled in the spectra and they don't overlap with peaks of interest. When there is uncertainty, we ran the CP experiment at multiple spinning frequencies to be certain of our peaks.

Note: The intrinsic heterogeneous nature of melanin biopolymer results in broad linewidth in the NMR spectra, which can't be improved with higher field, spinning or temperature of the experiments. Cross polarization experiment was chosen over spectral editing or direct polarization experiments due do to the fact that it is not useful/applicable in what we want to achieve and also not feasible due to the long acquisition time of the experiments.

H. Dynamic nuclear polarization (DNP) solid-state NMR spectroscopy. Dried melanin sample (30mg) was mixed with 20 mM AMUPol polarizing agent in d8-glycerol/D_2O/H_2O (60/30/10 v/v). The resulting mixture was packed in a 3.2 mm sapphire rotor and all experiments were acquired at ^{1}H frequency of 600 MHz at 100 K. An enhancement factor of ~20 was obtained on the samples. The 1D ^{15}N spectra of L-Tyr-melanin, TA-melanin, L-DOPA-melanin, and DA-melanin (Fig. 2) were acquired with 20k-36k scans. The 2D ^{13}C-^{13}C SPC5 spectrum of U-^{13}C,^{15}N-L-Tyr-melanin (Fig. 5) was acquired with a 3.5 s recycle delay, 512 scans per increment, and 64 t1 increments of 24 μs. The 2D ^{13}C-^{15}N TEDOR (Fig. 5) was acquired at 1.66 ms mixing time, 256 scans per increment, 64 t1 increments of 42 μs and a 3 s recycle delay. The 2D ^{13}C-^{13}C PDSD spectra (Supporting Fig. S15) was acquired at 10 ms, 50 ms, 100 ms, and 300 ms mixing times. Each PDSD was conducted with 256 scans, a 3.5 s recycle delay, and 128 t1 increments of 2 6μs.

I. Scanning electron microscopy (SEM). Dried melanin powder was placed on conductive carbon tape on an aluminum sample holder and coated using an iridium-sputter coating for 8 s. A FEI Quanta FEG 250 microscope was used for acquiring images using a 3-5 kV energy source with a spot size of 3 under high vacuum at a working distance of 9 mm.

J. Supporting Spectra. The following figures provide supporting spectral analyses and assignments.

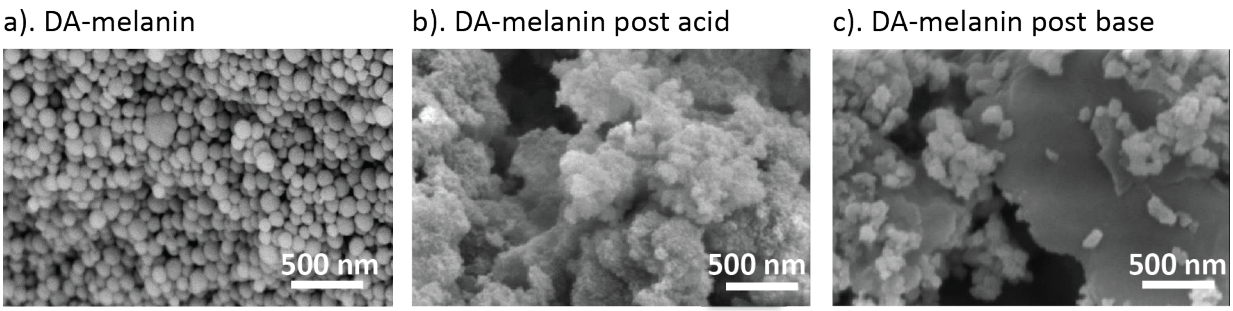

Figure S1. Comparisons of the method used in this paper with the conventional acid/base treatments of melanin nanoparticles shows that the method provided in this study does not result in destructions to the biopolymer. SEM images of dopamine-melanin treated with conditions used in this paper where: **a)** the resulting melanin is washed with neutral water,**, b)** the melanin particles were taken and washed with acid, neutralized with base to pH 7 followed by repeated washes with water or **c).** the melanin particles from **a)** were washed with base, neutralized with acid to pH 7 followed by repeated washed with water.

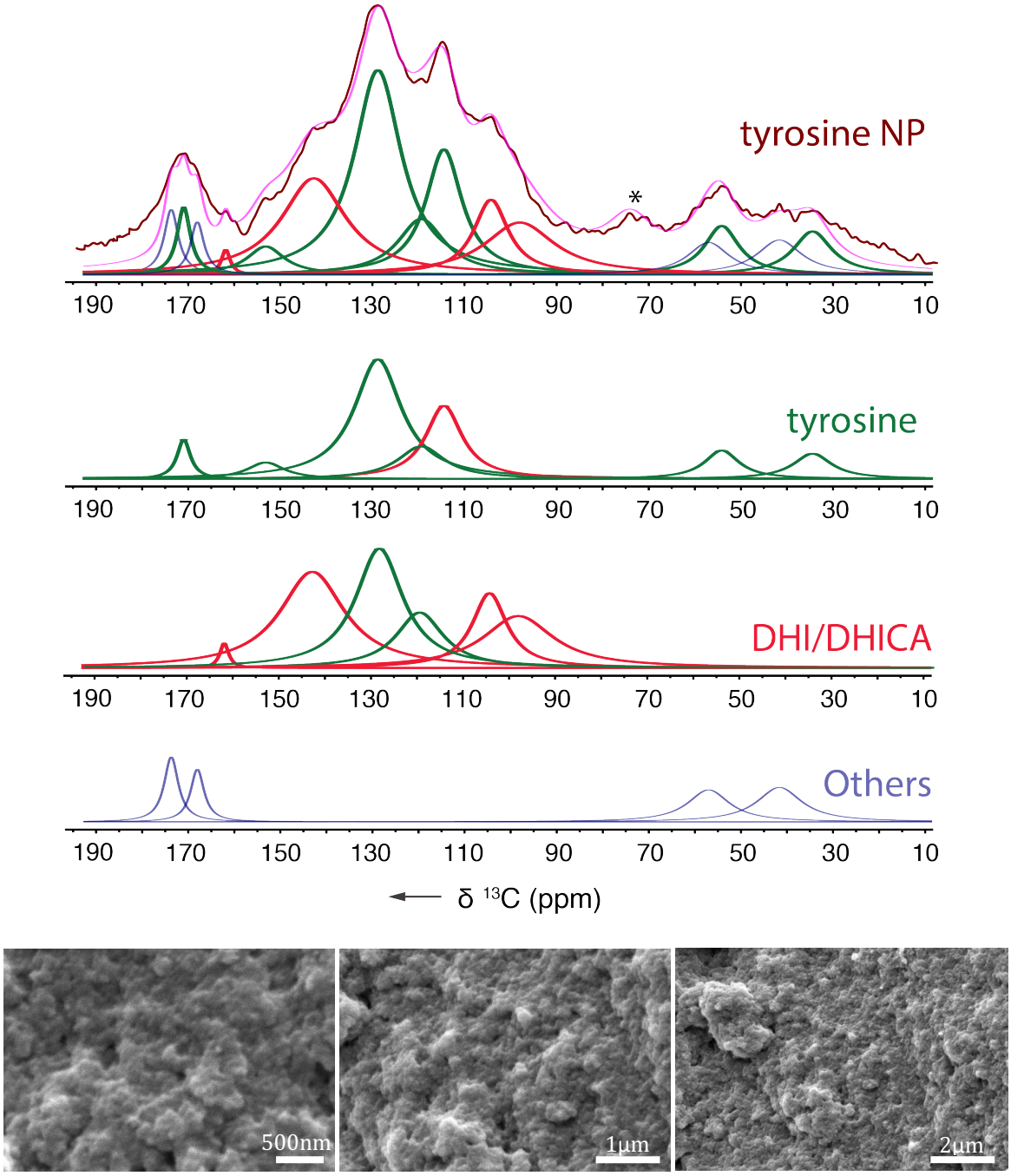

Figure S2. Spectral analysis of L-Tyr-melanin. (top) 1D ^{13}C spectrum of L-Tyr-melanin and deconvoluted peaks. There are at least three components that comprise L-Tyr-melanin. The first is peaks that follow pure tyrosine monomer units, second, are peaks containing chemical shift values that agree to those of DHI and DHICA units, and last, other components that have carbonyl and aliphatic moieties. (bottom) Select SEM images of L-Tyr-melanin at different magnifications.

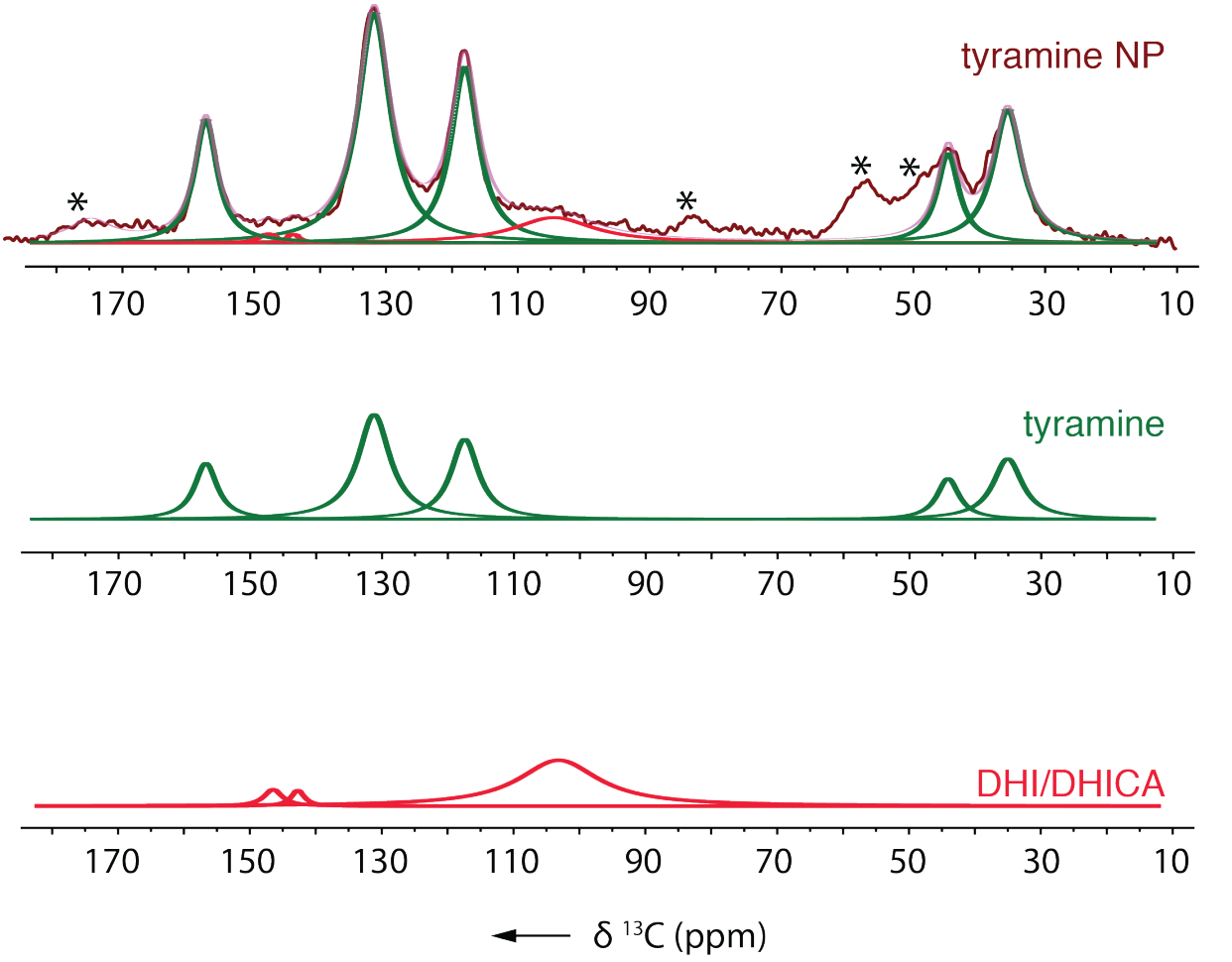

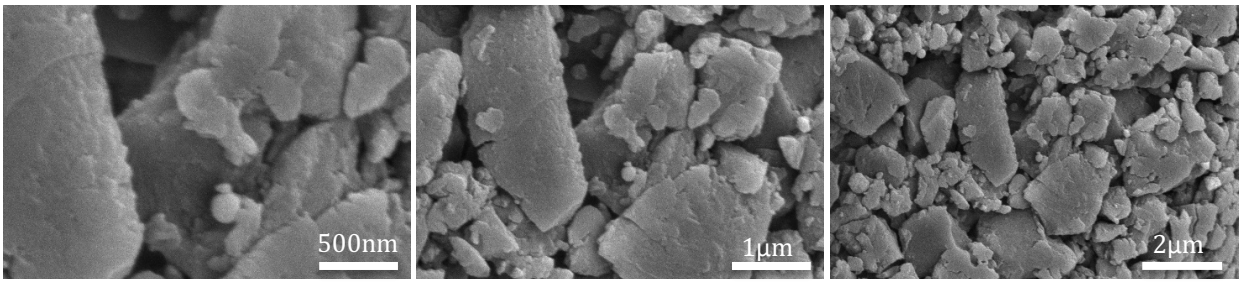

Figure S3. Spectral analysis of TA-melanin. (top) 1D ^{13}C of TA-melanin and its deconvoluted peaks. There are at least 2 components that comprise TA-melanin, peaks that follow pure tyramine monomer units and peaks containing chemical shift values that agree to those of DHI and DHICA units. (bottom) SEM images of TA-melanin at different magnifications.

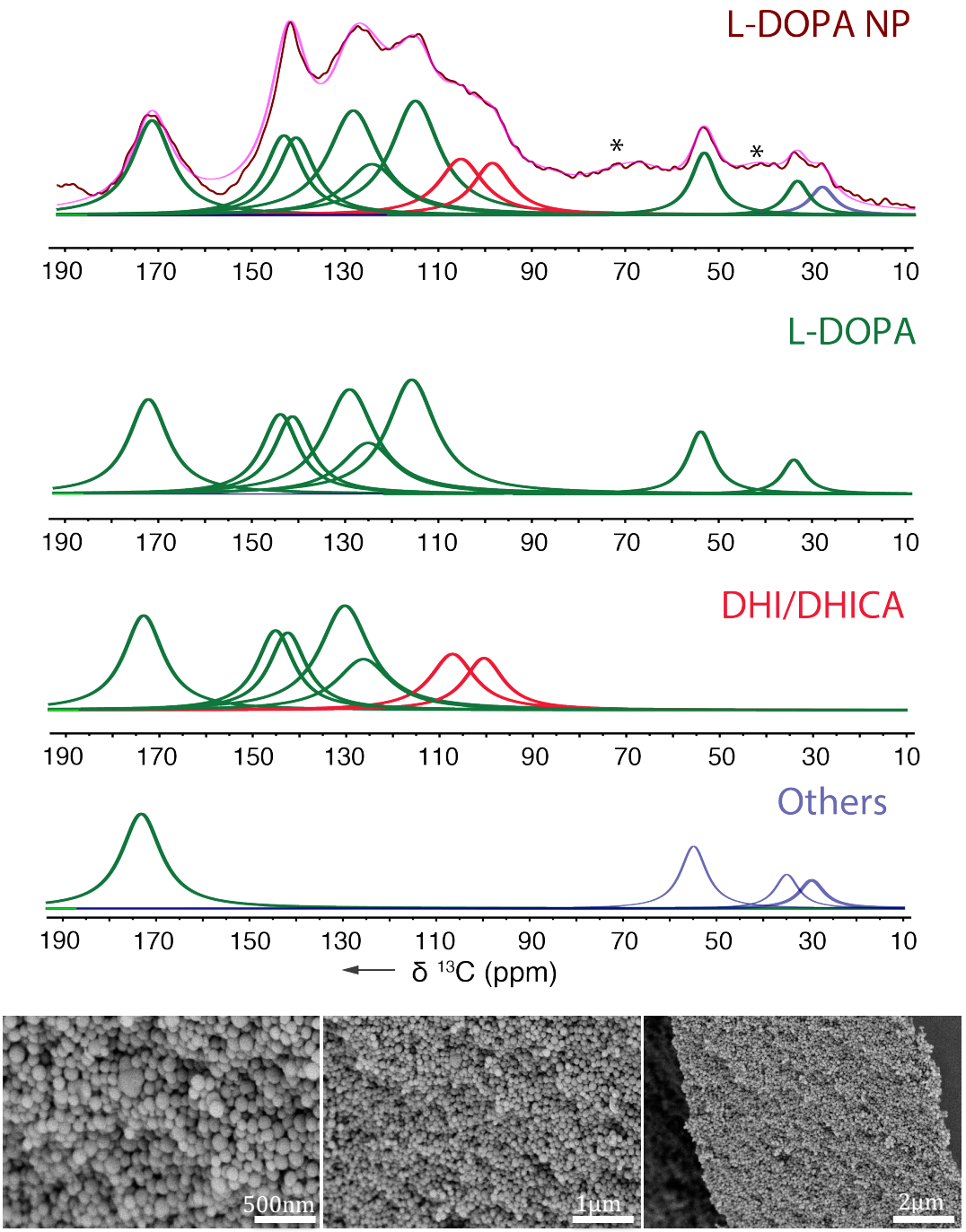

Figure S4. Spectral analysis of L-DOPA-melanin. (top) 1D ^{13}C of L-DOPA-melanin and its deconvoluted peaks. There are at least 3 components in L-DOPA-melanin, peaks that follow pure tyrosine monomer units, peaks containing chemical shift values that agree to those of DHI and DHICA units, and last, other components that have carbonyl and aliphatic moieties. (bottom) SEM images of L-DOPA-melanin at different magnifications.

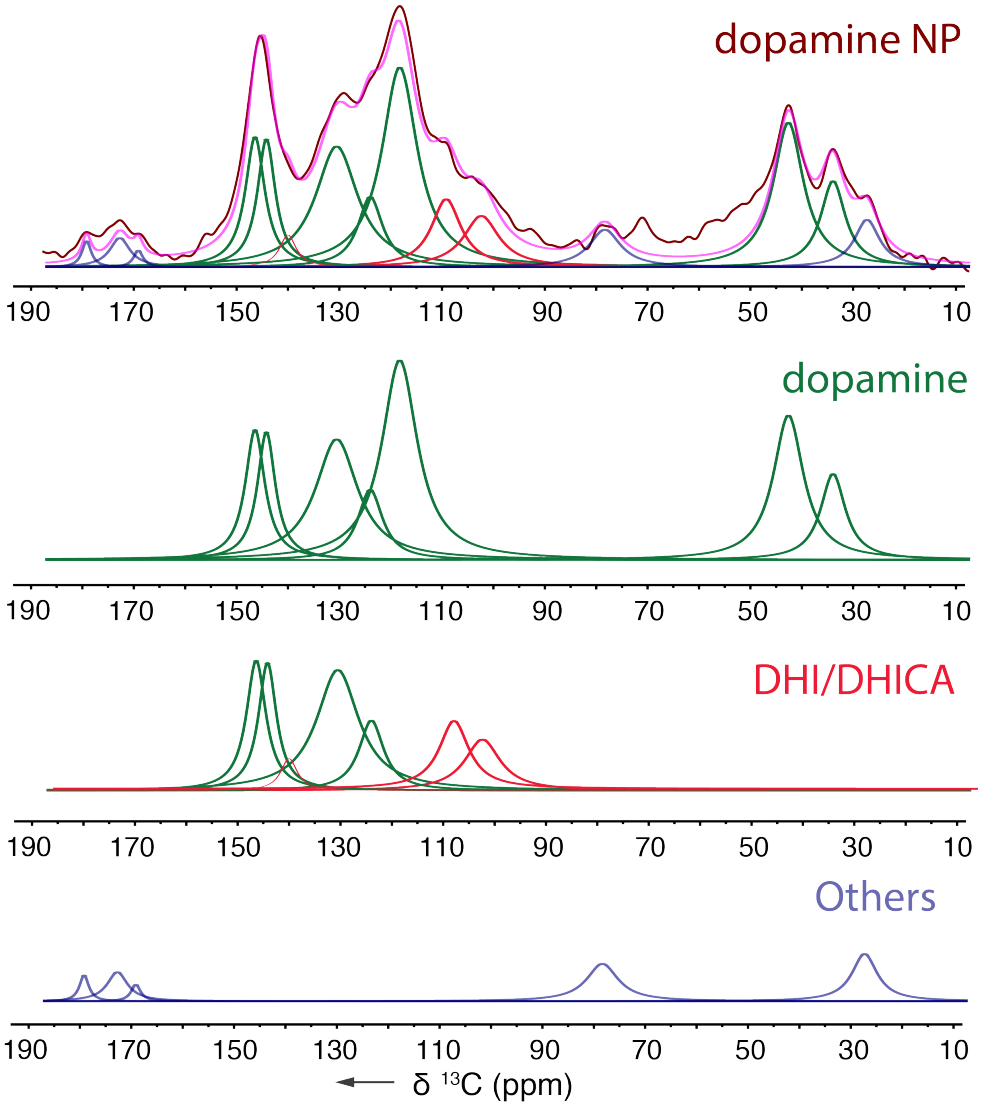

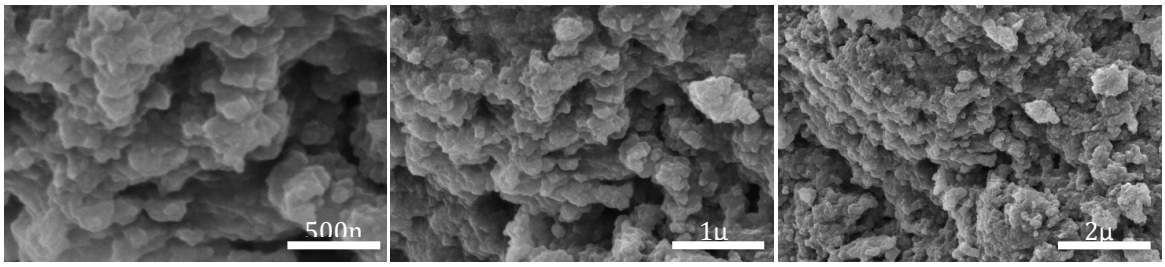

Figure S5. Spectral analysis of DA-melanin. (top) 1D ^{13}C of DA-melanin and its deconvoluted peaks. There are at least three components that comprise DA-melanin, peaks that follow pure tyrosine monomer units, peaks containing chemical shift values that agree to those of DHI and DHICA units, and last, other components with carbonyl and aliphatic moieties. (bottom) SEM images of DA-melanin at different magnifications.

tyrosine	tyramine	L-dopa
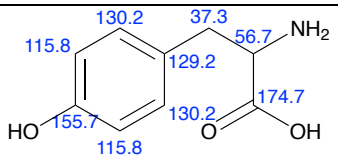	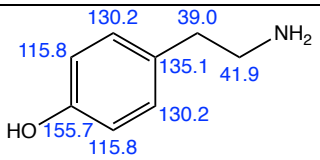	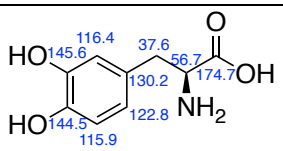
dopamine	**DHICA**	**DHI**
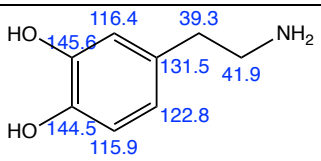	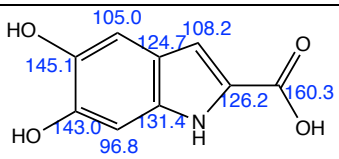	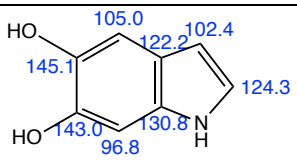
dopaquinone	**leucochrome**	**dopachrome**
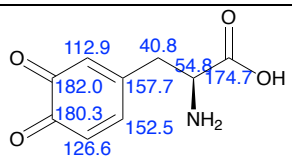	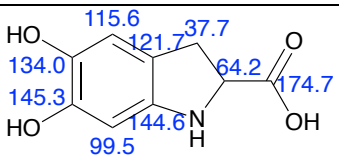	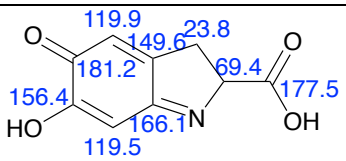

Figure S6. ^{13}C chemical shift predictions for metabolites within Raper-Mason pathway generated using ChemNMR in ChemDraw v.18.0 (Perkin-Elmer). These predictions were used to analyze our experimental data. Although some of the chemical values of a few carbons of metabolites on aromatic ring are similar, but each metabolite contains a set of unique chemical shift values that they can be used to match perfectly with the experimental melaninised chemical shift values.

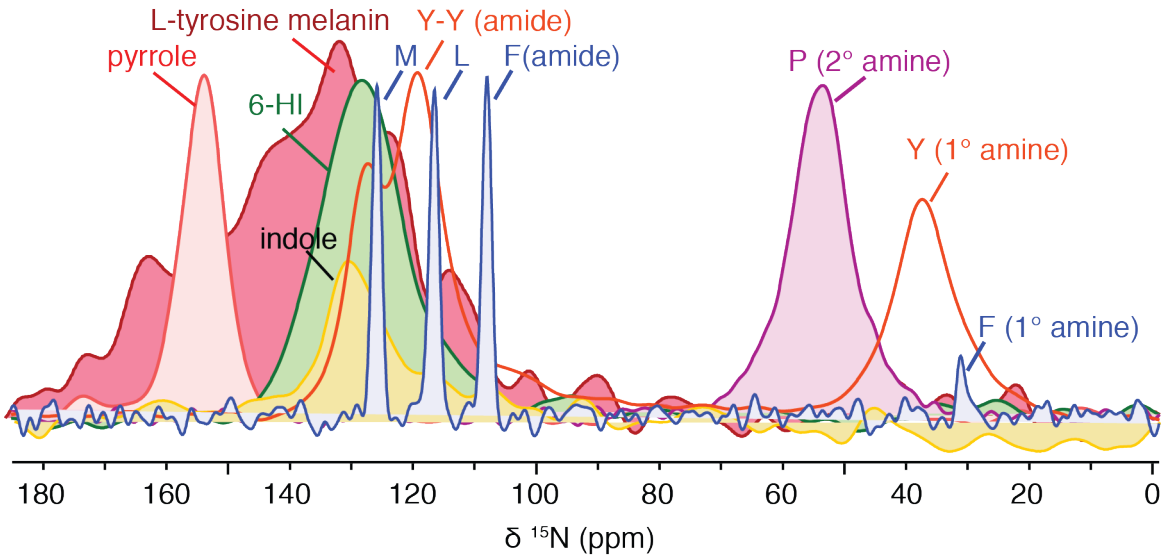

Figure S7. 1D ^{15}N CP DNP MAS NMR spectra of the nitrogen standards overlaid with melanised L-tyrosine. This is the method used in this manuscript to analyze the various possible nitrogen components in the melanised precursor monomers.

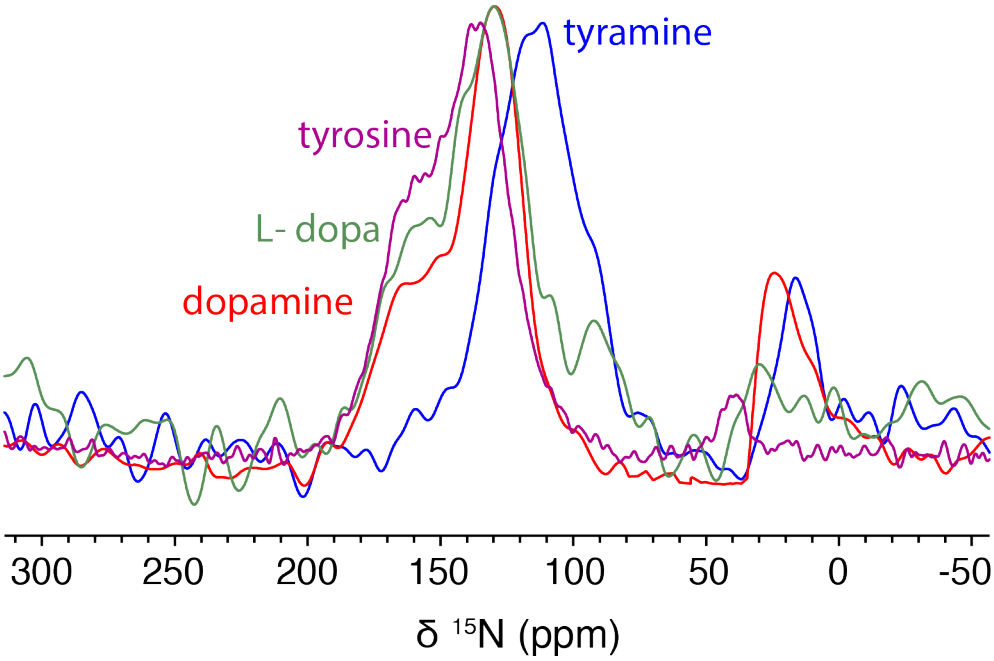

Figure S8. 1D ^{15}N CP DNP MAS NMR spectral overlay of L-Tyr-melanin, TA-melanin, L-DOPA-melanin, and DA-melanin. The peaks originate from pyrrole, indole, hydroxyindole, amide, and primary amine groups at ~δ 160 ppm, 135 ppm, 115 ppm and 22 ppm respectively. The chemical shifts of nitrogen standards are shown in Figure S6. Out of the four melanins, TA-melanin (blue) is the most upfield and is the only sample without a pyrrole shoulder peak at ~δ 160 ppm. All samples had a primary amine peak at ~δ 35 ± 10 ppm.

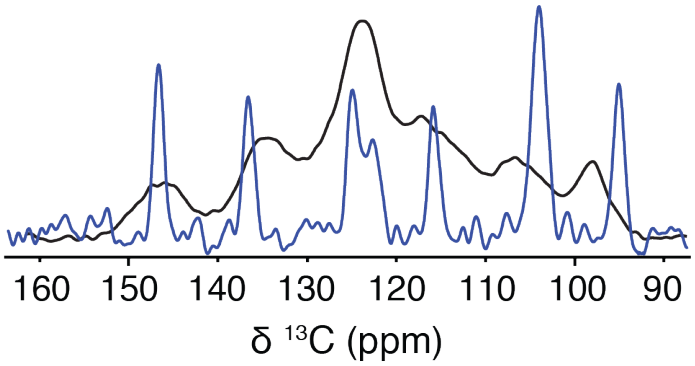

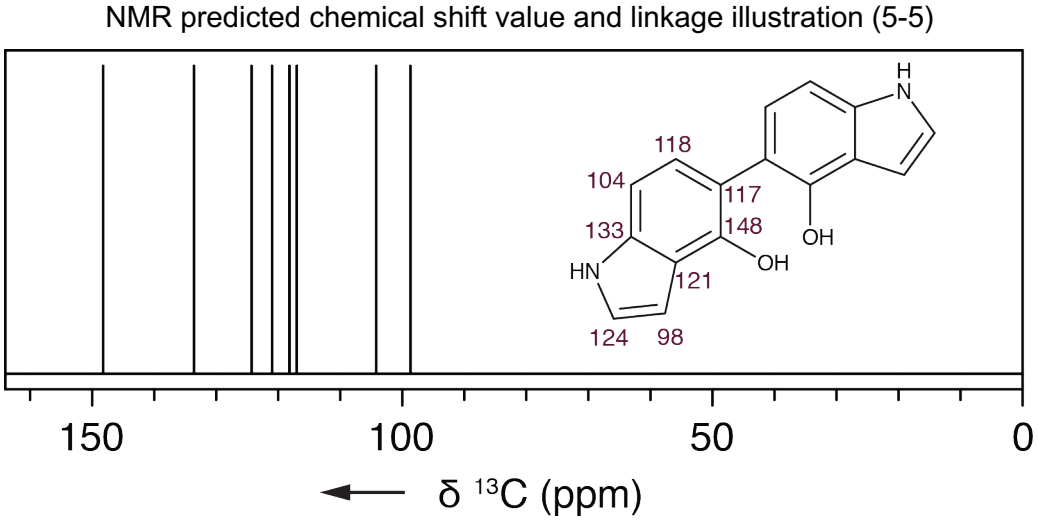

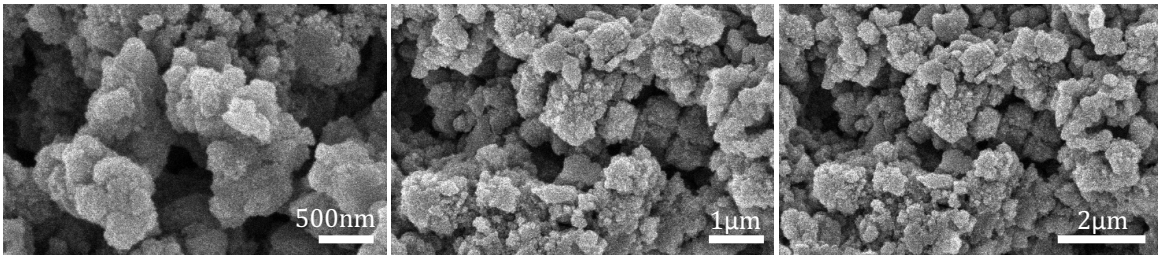

Figure S9. Spectral analysis of 4-HI-melanin. (top) 1D ^{13}C NMR of 4-HI-melanin (black) is overlaid with 4-HI monomer (blue). (middle) Using concepts of symmetric *versus* asymmetric linkage and chemical shift predictions using ChemNMR in ChemDraw v.18.0 (Perkin-Elmer). All possible linkage combinations were drawn, and its chemical shifts were predicted. The one that matched the most with our experimental data was taken. We conclude a linkage of 5-5 between the 4-HI monomer. (bottom) SEM images of 4-HI-melanin at different magnifications.

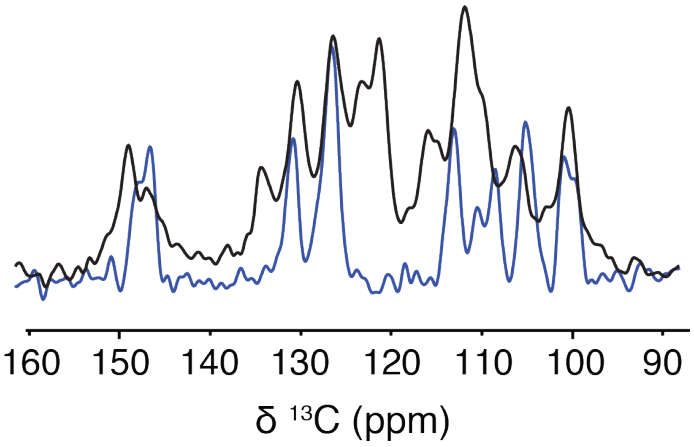

NMR predicted chemical shift value and linkage illustration (2-4)

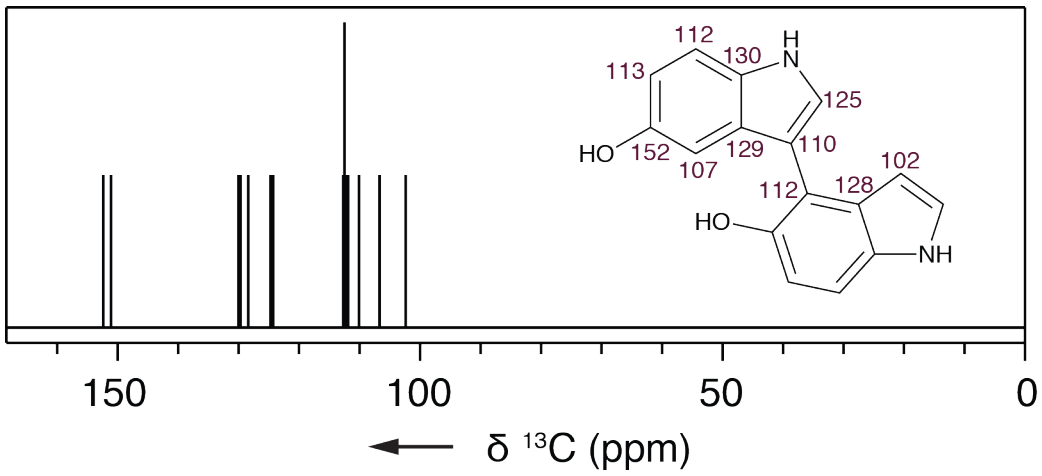

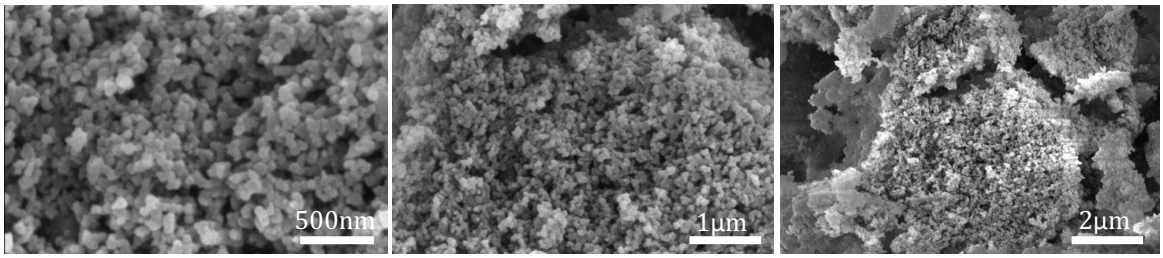

Figure S10. Spectral analysis of 5-HI-melanin. (top) 1D ^{13}C NMR of 5-HI-melanin (black) is overlaid with 5-HI monomer (blue). (middle) Using concepts of symmetric *versus* asymmetric linkage and chemical shift predictions using ChemNMR in ChemDraw v.18.0 (Perkin-Elmer). All possible linkage combinations were drawn, and its chemical shifts were predicted. The one that matched the most with our experimental data was taken. We conclude a linkage of 2-4 between the 5-HI monomers. (bottom) SEM images of 5-HI-melanin at different magnifications.

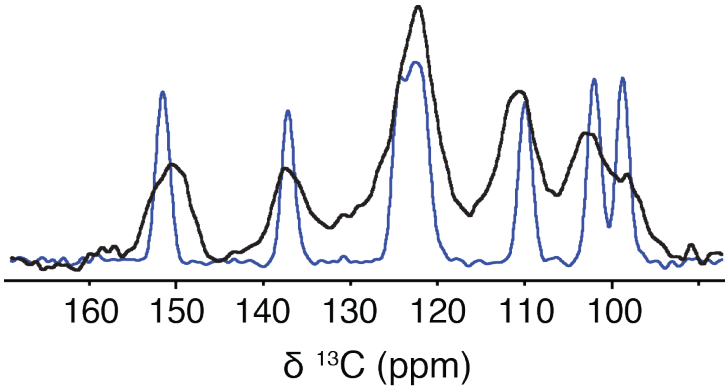

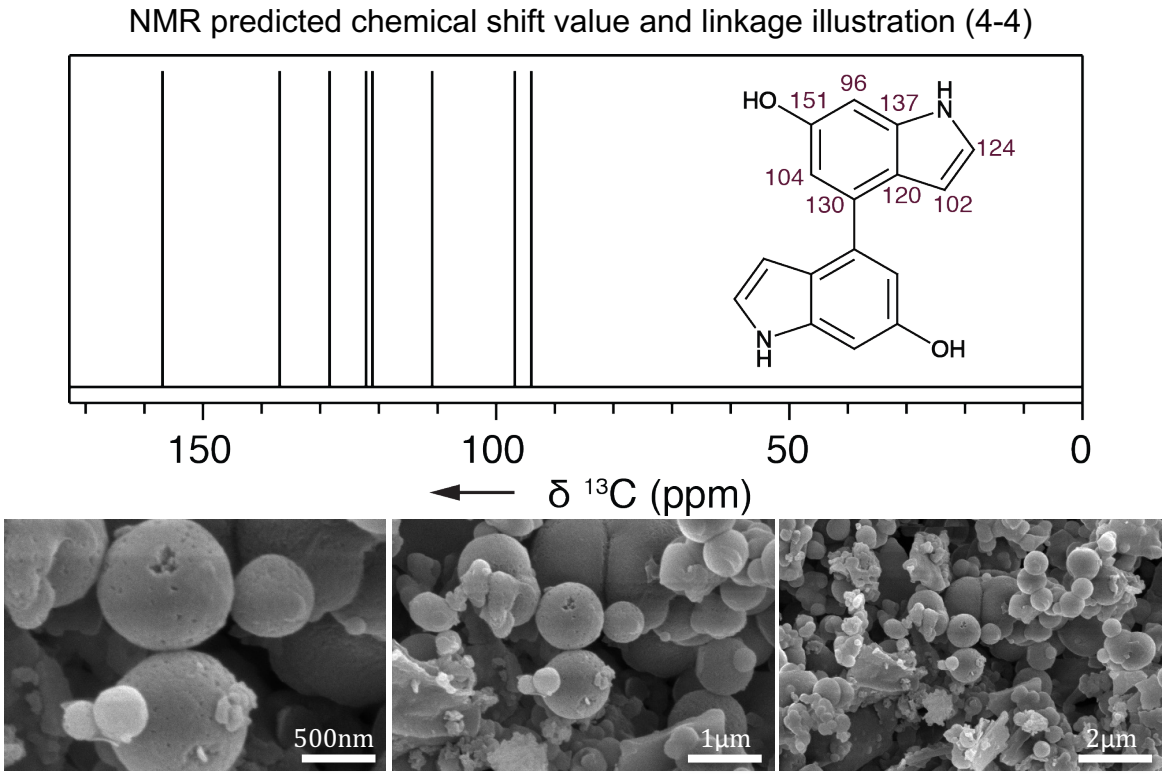

Figure S11. Spectral analysis of 6-HI-melanin. (top) 1D ^{13}C NMR of 6-HI-melanin (black) is overlaid with 6-HI monomer (blue). (middle) Using concepts of symmetric *versus* asymmetric linkage and chemical shift predictions using ChemNMR in ChemDraw v.18.0 (Perkin-Elmer). All possible linkage combinations were drawn, and its chemical shifts were predicted. The one that matched the most with our experimental data was taken. We conclude a linkage of 4-4 between the 6-HI monomers. (bottom) SEM images of melanised 6-HI at different scales are shown.

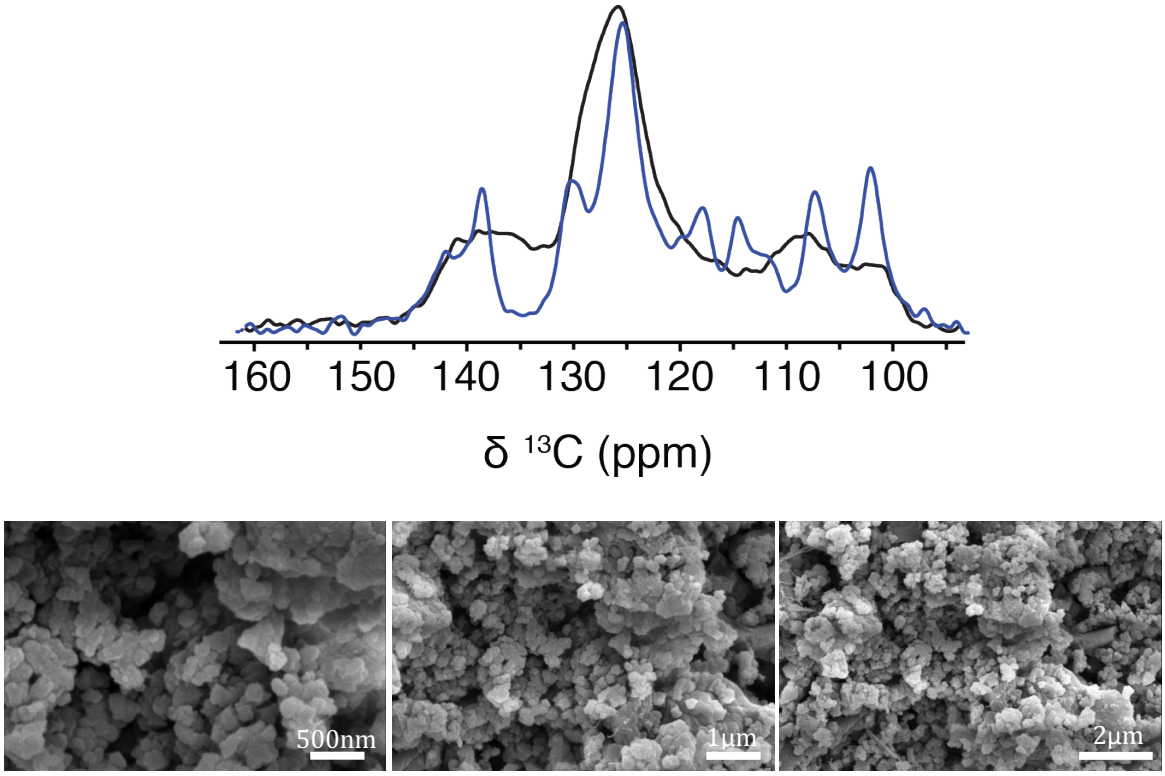

Figure S12. Spectral analysis of 7-HI-melanin. (top) 1D ^{13}C NMR of 7-HI-melanin (black) is overlaid with 7-HI precursor (blue). All possible linkage combinations were drawn, and its chemical shifts were predicted using ChemNMR in ChemDraw v.18.0 (Perkin-Elmer). Due to the broadness of the melanised 7-HI peaks, there are several possibilities of linkage between the 7-HI monomer groups. (bottom) SEM images of melanised 7-HI at different scales are shown.

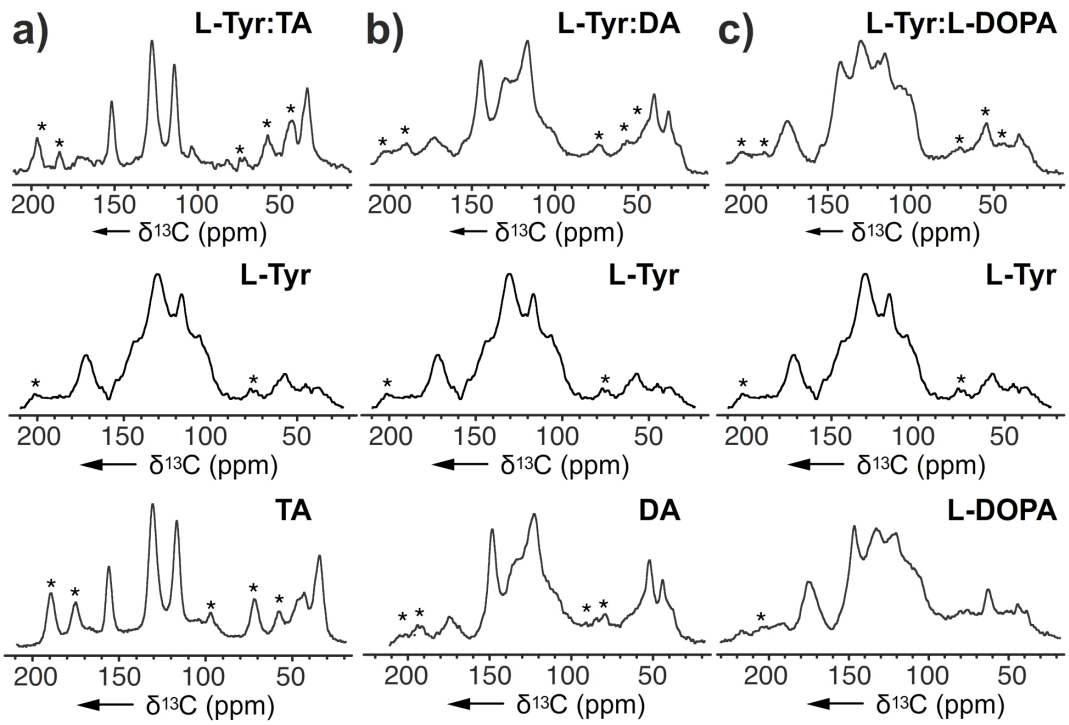

Figure S13. 1D ^{13}C NMR of melanin produced by copolymerizing two monomers: **a)** L-Tyr:TA melanin generated from a mixture of L-Tyr and TA, **b)** L-Tyr:L-DA melanin, **c)** L-Tyr:L-DOPA melanin using *A. bisporus* tyrosinase. Comparison of the NMR spectra of these mixtures to that of its pure monomers (shown below the copolymers) offers insight into the monomer selectivity of this enzyme. This figure is provided as supporting information for Fig. 4a-4c in the manuscript where panels a-c in Fig. S13 supports panel a-c in Fig. 4.

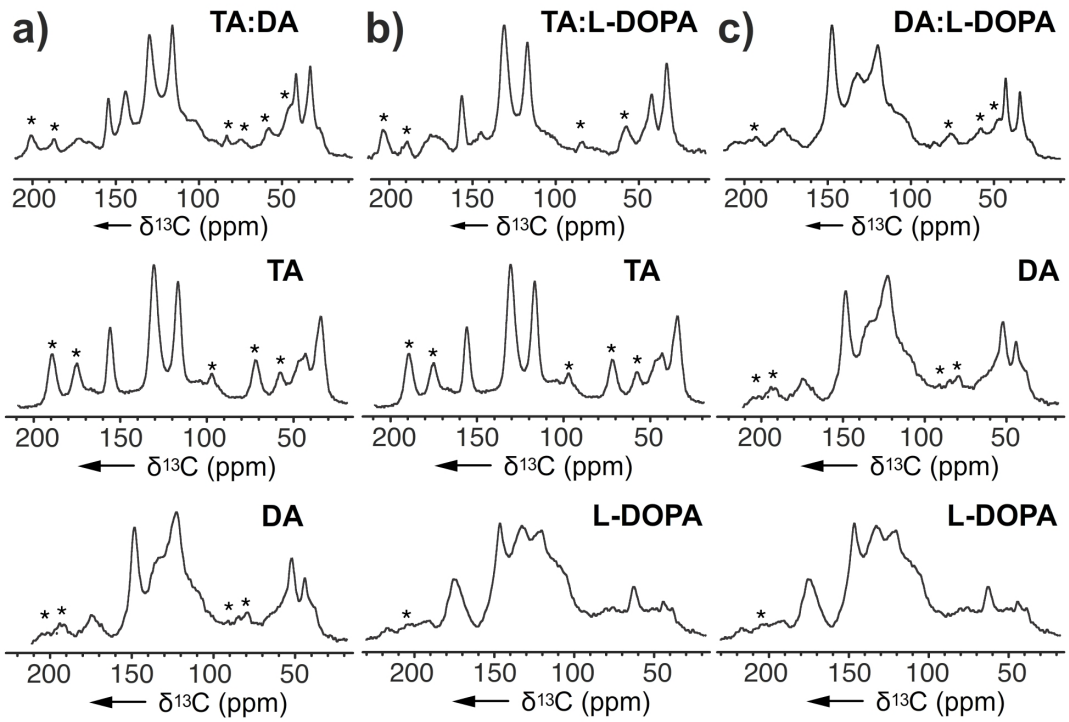

Figure S14. 1D ^{13}C NMR of melanin produced by copolymerizing two monomers: a) TA:DA melanin, b) TA:L-DOPA melanin, and c) DA:L-DOPA melanin using *A. bisporus* tyrosinase. Comparison of the NMR spectra of these mixtures with that of pure monomers (Fig. 2) was used to explore the monomer selectivity of this enzyme. This figure is provided as supporting information for Fig. 4d-4f in the manuscript where panels a-c in Fig. S14 supports panel d-f in Fig. 4.

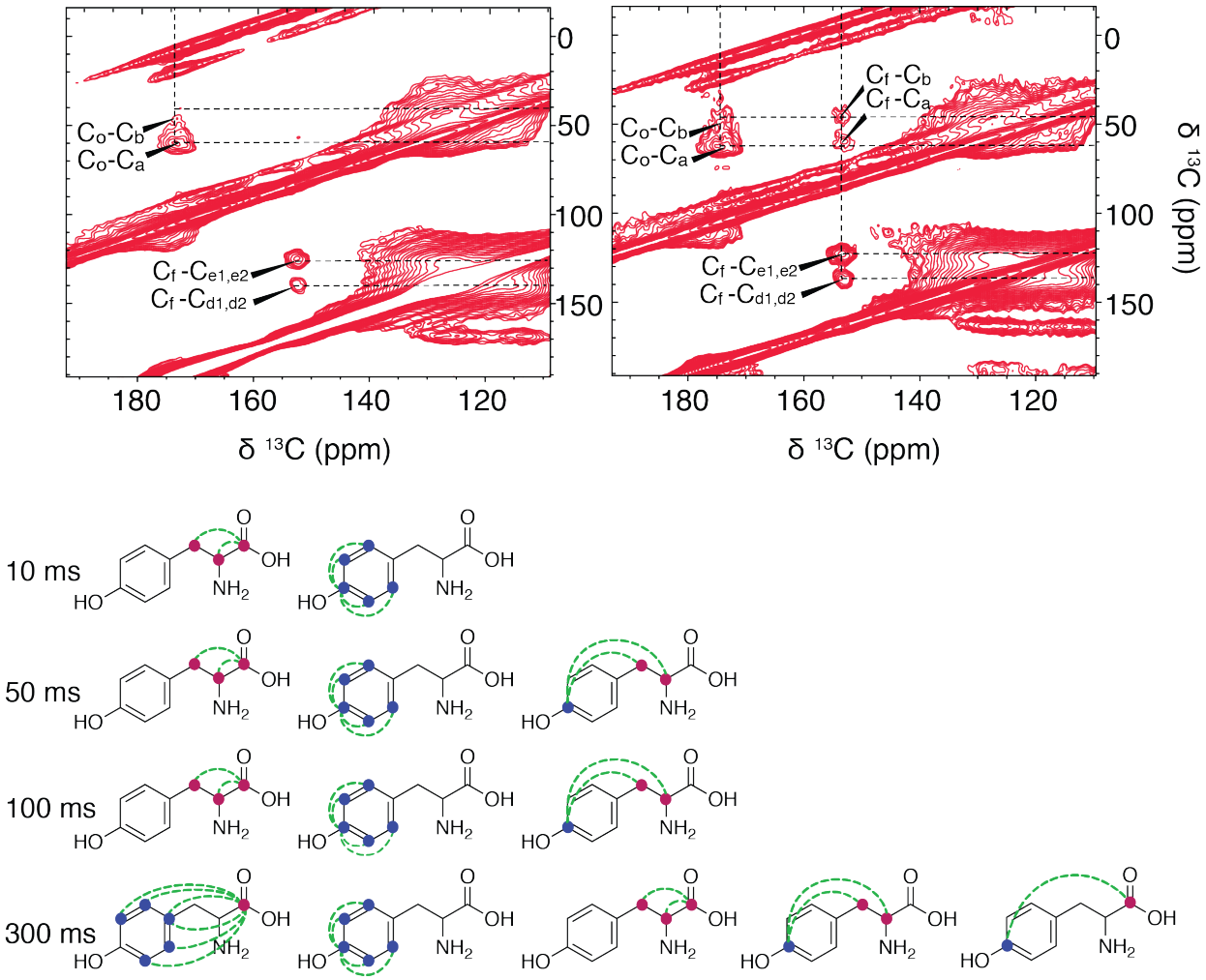

Figure S15. 2D DNP NMR analyses of U-^{13}C,^{15}N-L-Tyr-melanin. (top) 2D ^{13}C-^{13}C PDSD spectra of U-^{13}C,^{15}N-L-Tyr-melanin showing the correlations between the atoms in the polymer at 10 ms (left) and 100 ms (right) mixing times. (bottom) Observed correlations are depicted on the tyrosine monomer as a function of mixing times. The order of appearance of the correlations is drawn according to the intensity of the contour peaks with respect to each other from strongest to weakest. The observed correlations are mostly due to intramolecular correlations instead of intermolecular correlations, with the exception of possible intermolecular interactions between stacked tyrosine units.

Note: The molecules that are of higher population are more likely to be detected by NMR. Not all molecules in a system are going to be detected by NMR especially given the broadness of the peaks, and PDSD doesn't guarantee all components of the sample will be detected, which is why we have combined our PDSD analysis with SPC5 data (Figure 5A). We tackled the C-C relationship through both through-space and through-bond experiments to obtain as much information as we can with the given technology. The DHI and DHICA units were detected in SPC5, which confirms the conclusion from Fig. S2.

K. Additional Discussion. The significance of many possibilities for structural diversity in eumelanin pigments explains why there are different variations of melanin in nature.

The sequential progression of intermediates in the Raper-Mason model is an oversimplification that has not been addressed in the literature thus far. As such, our findings open a new avenue for the exploration of the substantially nuanced Raper-Mason pathway that was previously based on simple sequential progression.

Other decarboxylase steps were mentioned in Scheme 1 to point out there are many other enzymes present *in vivo*, and which can each effect the output melanin.

In the past, very limited studies have been done on the selectivity of tyrosinase, for example, Nistora and coworkers[S1] use the tyrosinase as a biosensor in electrodes. In a second example, Florescu and coworkers[S2] focus on a tyrosinase-based biosensor developed to detect dopamine. None of the studies focused on the enzyme's selectivity for the different metabolites in the Raper-Mason pathway, nor the selectivity for unnatural substrates that could be present as shown in Fig. 3 (4-HI, 5-HI, 6-HI, and 7-HI) and how all these alter the melanin's structure.

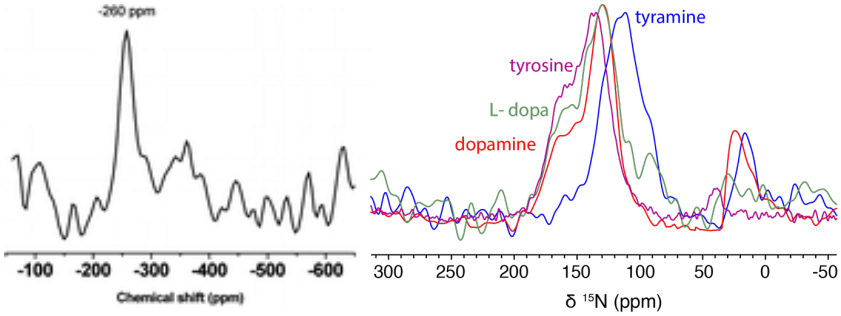

Figure S16. (left) Solid state ^{15}N NMR spectra of poly(dopamine) (400 MHz, spinning rate: 6 kHz).[S4] (right) The ^{15}N NMR spectrum of the four precursor melanins (Tyrosine NP, tyramine NP, L-dopa NP and dopamine NP) presented in this study acquired with DNP (600 MHz, spinning rate: 12.5 kHz).

It should be noted that the melanin polymers prepared in this study were prepared using different methods than those previously reported in the literature.[S3] Previous protocols involve washing the melanin polymer with harsh 6 M HCl after being polymerized, "The reaction mixture was then brought to pH 1 by addition of 6 M HCl and boiled for 20 min." This additional step destroys the overall pigment structure shown in Figure S1, while our approach of thoroughly washing the polymers with H_2O is noninvasive. This explains why our 2D NMR spectra and the conclusions drawn from this study are different from what has been published.

L. Additional References

S1 C. Nistora. J. Emnéus. L. Gorton, A. Ciucub, Improved stability and altered selectivity of tyrosinase based graphite electrodes for detection of phenolic compounds. *Anal. Chim. Acta.* 1999, ***387***, 309-326.

S2. M. Florescu, D. David, Tyrosinase-Based Biosensors for Selective Dopamine Detection. *Sensors (Basel).*2017, ***17***, 1314

S3. S. Chatterjee, R. Prados-Rosales, S. Tan, V. C. Phan, C. Chrissian, B. Itin, H. Wang, A. Khajo, R. S. Magliozzo, A. Casadevall, R. E. Stark, The melanization road more traveled by: Precursor substrate effects on melanin synthesis in cell-free and fungal cell systems. *J. Biol. Chem.* 2018, ***293***, 20157-20168.

S4. D. R. Dreyer, D. Miller, B. Freeman, D. R. Paul, C. W. Bielawski, Elucidating the structure of poly(dopamine). *Langmuir,* 2002, ***28***, 6428-6435.